Global profiling of toxicologically relevant metabolites in urine: case study of reactive aldehydes

Emilien L. Jamin, Robin Costantino, Loïc Mervant, Jean-Francois Martin,
Isabelle Jouanin, Florence Blas-Y-Estrada, Françoise Guéraud, Laurent
Debrauwer

HAL Id: hal-02622690
https://hal.inrae.fr/hal-02622690

Submitted on 26 May 2020

Article

Global profiling of toxicologically relevant metabolites in urine: case study of reactive aldehydes

Emilien L Jamin, Robin Costantino, Loïc Mervant, Jean-Francois Martin, Isabelle JOUANIN, Florence Blas-Y-Estrada, Françoise Guéraud, and Laurent Debrauwer

Just Accepted

Comment citer ce document :
Jamin, E. (Auteur de correspondance), Costantino, R., Mervant, L., Martin, J.-F., Jouanin, I., Blas-Y-Estrada, F., Guéraud, F., Debrauwer, L. (2020). Global profiling of toxicologically relevant metabolites in urine: case study of reactive aldehydes. Analytical Chemistry, 92 (2), 1746-1754. , DOI : 10.1021/acs.analchem.9b03146

1 **Global profiling of toxicologically relevant metabolites in urine: case study of**

2 **reactive aldehydes**

3

4 Emilien L. Jamin*°(1)(2), Robin Costantino*(1)(2), Loïc Mervant(1)(2), Jean-François Martin(1)(2),

5 Isabelle Jouanin(1)(2), Florence Blas-y-Estrada(2), Françoise Guéraud*(2) and Laurent

6 Debrauwer*(1)(2)

7

8 (1) Metatoul-AXIOM platform, National Infrastructure for Metabolomics and Fluxomics: MetaboHUB,

9 Toxalim, INRAE, 31300 Toulouse, France

10 (2) Toxalim (Research Centre in Food Toxicology), Toulouse University, INRAE UMR 1331, ENVT, INP-

11 Purpan, UPS, 31300 Toulouse, France.

12 * Equal contribution

13 ° Corresponding author: emilien.jamin@inra.fr

14

15 **Abstract**

16 Among the numerous unknown metabolites representative of our exposure, focusing on toxic

17 compounds should provide more relevant data to link exposure and health. For that purpose, we

18 developed and applied a global method using data independent acquisition (DIA) in mass spectrometry

19 to profile specifically electrophilic compounds originating metabolites. These compounds are most of

20 the time toxic, due to their chemical reactivity towards nucleophilic sites present in bio-

21 macromolecules. The main line of cellular defense against these electrophilic molecules is conjugation

22 to glutathione, then metabolization into mercapturic acid conjugates (MACs). Interestingly, MACs

23 display a characteristic neutral loss in MS/MS experiments, that makes possible to detect all the

24 metabolites displaying this characteristic loss, thanks to the DIA mode, and therefore to highlight the

25 corresponding reactive metabolites. As a proof of concept, our workflow was applied to the

26 toxicological issue of the oxidation of dietary polyunsaturated fatty acids, leading in particular to the

1

27 formation of toxic alkenals, which lead to MACs upon glutathione conjugation and metabolization. By

28 this way, dozens of MACs were detected and identified. Interestingly, multivariate statistical analyses

29 carried out only on extracted HRMS signals of MACs yield a better characterization of the studied

30 groups compared to results obtained from a classic untargeted metabolomics approach.

31

32 **TABLE OF CONTENTS GRAPHIC**

33

34

2
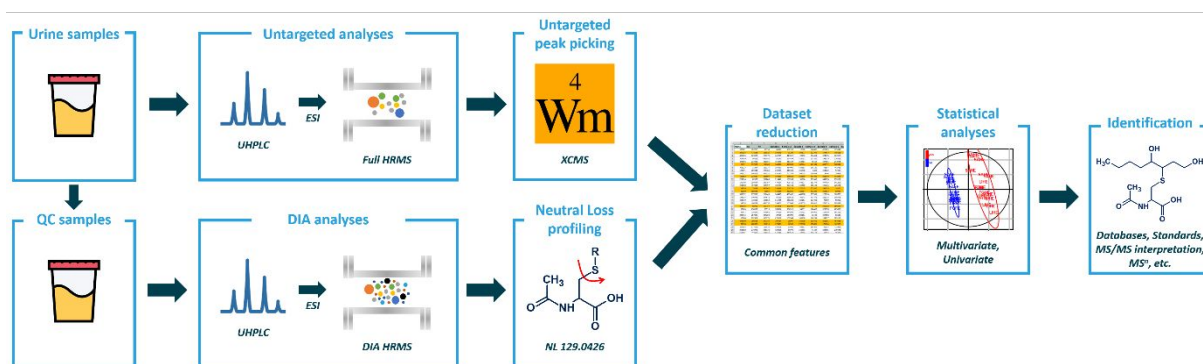
35   **INTRODUCTION**

36   Throughout their lives, humans are exposed to many substances, natural or not, in varying amounts

37   depending on their environment, lifestyle or diet. In particular through diet, people are exposed to a

38   wide variety of compounds mostly essential (*e.g.* nutrients, vitamins, etc…), but also, in a much lesser

39   extent, to compounds with possible harmful effects such as pesticides,[1] mycotoxins,[2] or neo-formed

40   compounds produced during the processing, cooking and digestion of food.[3] Since the concept of

41   exposomics has been introduced,[4] new approaches aim at assessing this exposure in the most

42   comprehensive way by the implementation of untargeted methods.[5] However, in front of the number

43   and complexity of these contaminants representing our chemical exposome, focusing on toxic

44   compounds appears essential to estimate the impact of this exposure on health. Many of these

45   toxicologically relevant compounds are toxic due to their electrophilicity, which makes them reactive

46   towards nucleophilic sites of biomolecules such as DNA, RNA, proteins…, and lead to the formation of

47   various adducts with potential harmful effects. Structure-activity relationships analyses carried out by

48   Ashby and Tennant[6] on the basis of carcinogenesis data from US-NTP showed that more than 80% of

49   genotoxic agents are electrophilic compounds or compounds that are able to be bioactivated into

50   electrophilic metabolites. In particular, meat represents a complex matrix that may contain a variety

51   of contaminants, some of which being involved in colon cancer development according to a commonly

52   accepted hypothesis involving the formation of DNA adducts.[7,8]

53   In terms of food safety, the cooking of meat at high temperature induces the formation of numerous

54   electrophilic compounds from heterocyclic amines (HCAs) and polycyclic aromatic hydrocarbons

55   (PAHs), such as 2-amino-3,8-dimethylimidazo-[4,5-*f*]-quinoxaline (MeIQx) or benzo[a]pyrene (BaP),

56   respectively, which are known to be pro-mutagenic by giving rise to DNA adducts after the formation

57   of reactive metabolites.[9] Alternatively, curing processes lead to the formation of *N*-nitroso compounds

58   (NOCs).[10] Some of these NOCs are known to be mutagenic because of their ability to form DNA

59   adducts.[11] Finally, several studies showed convincing evidence that heme iron contained in red meat,

60   could be one of the main factors of carcinogenesis promotion.[12–14] The main hypothesis to explain

3

61   heme iron toxicity relies on its ability to promote the formation of radical species by Fenton-like

62   reactions, which leads to the peroxidation of dietary polyunsaturated fatty acids into secondary lipid

63   peroxidation electrophilic products such as 4-hydroxynonenal (4-HNE).[15] As reported by Sesink et al.[16]

64   and further confirmed by Bastide et al.,[17] heme-iron as such does not participate to carcinogenesis

65   promotion, which is mainly mediated through lipid peroxidation product formation in the colon lumen.

66   Targeted methods are commonly used to monitor these reactive metabolites, able to covalently bind

67   to biomolecules.[18] Concerning lipid peroxidation, 4-HNE has been one of the most studied lipid

68   peroxidation secondary product.[19–21] However, depending on the fatty acid precursor, lipid

69   peroxidation may induce the formation of many other reactive compounds (potentially unknown) with

70   various abundance and reactivity. Developing untargeted methods are then necessary to get a more

71   comprehensive view of their formation.

72   One of the main detoxification routes employed to detoxify such reactive/electrophilic compounds is

73   the enzymatic conjugation with glutathione, a tripeptide known as an efficient scavenger of

74   electrophilic species. Those glutathione conjugates are then cleaved by γ-glutamyltransferase and

75   cysteinylglycine dipeptidase, respectively, and finally *N*-acetylated to form mercapturic acid conjugates

76   (MACs) that are mostly urine-excreted.[22] Thus, MACs are the result of detoxification processes of

77   reactive electrophilic species and can be considered as biomarkers of exposure to these harmful

78   compounds. Monitoring MACs could therefore be useful for a more accurate characterization of

79   exposure to reactive compounds and a better evaluation of the role of reactive metabolites in

80   toxicology in general.[23]

81   Despite the interest of this approach, only a few studies have focused on the global analysis of MACs.[24–]

82   [26] These studies aimed at evaluating the electrophilic burden of the organism by screening

83   mercapturates in an untargeted way by liquid chromatography coupled with mass spectrometry (LC-

84   MS) using constant neutral loss-like acquisition mode. Other available studies of MACs were based on

85   MS targeted analysis to study specific exposure situations like atrazine[27] or neo-formed products in

86   food such as acrylamide or acrolein.[28] All these works use the characteristic loss of 129 Da observed

4

87   from MACs in urine samples by the cleavage of the thioether bond, and rely on low-resolution mass

88   spectrometry.

89   In the present study, we present an original method for the global screening of MACs. A high-resolution

90   mass spectrometry (HRMS) based workflow was developed using a data-independent acquisition

91   mode (DIA) for monitoring the specific neutral-loss of mercapturates through gas phase fragmentation

92   in mass spectrometry. As a proof of concept, this paper presents results from a study based on an

93   animal experiment conducted with different diets containing various oils (fish oil, safflower oil and

94   hydrogenated coconut oil) with different polyunsaturated fatty acids profiles, in combination with

95   heme iron to catalyze lipid peroxidation. Thus, monitoring urinary MACs in these animals provided an

96   accurate overview of their exposure to lipid peroxidation products conjugated with glutathione.

97   **EXPERIMENTAL SECTION**

98   **Chemicals**

99   All solvents were purchased from Fisher Scientific (Thermo Fisher Scientific, Illkirch, France) and were

100   LC-MS grade. Standard 4-hydroxynonan-1-ol mercapturic acid (DHN-MA), 4-hydroxyoctan-1-ol-MA, 4-

101   hydroxyheptan-1-ol-MA, 4-hydroxyhexan-1-ol-MA (DHH-MA), 4-hydroxynonanal-MA, 4-

102   hydroxyoctanal-MA and 4-hydroxyheptanal-MA, were synthetized in the laboratory as previously

103   described[29]. Standard *N*-acetyl-*S*-phenylcysteine was purchased from Sigma-Aldrich (Saint Quentin

104   Fallavier, France) and the MS calibration mix solution was purchased from Waters (Manchester, UK).

105   Heme iron (Hemin from bovine) was purchased from Sigma-Aldrich, and fish oil (Refined Menhaden

106   oil), safflower oil and hydrogenated coconut oil came from MP Biomedicals (Illkirch-Graffenstaden,

107   France).

108   **Animals and diets**

109   Young adults Fischer male rats (6 rats/group) were housed individually in plastic metabolic cages. They

110   were allowed for 3 days of acclimatization to their cage. The room was kept at a temperature of 22 °C

111   on a 12h light-dark cycles. Animals had free access to tap water and to their respective diet for 15 days.

112   Diets were given each day at the end of the afternoon in order to limit oxidation, and 24h-urine

5

113   samples were collected at day 12 and frozen (-20°C) until analysis. A first set of diets contained 5% fish

114   oil (containing long chain ω-3 fatty acids). A second set of diets contained 5% safflower oil (containing

115   ω-6 fatty acids). A last set of control diets contained 5% hydrogenated coconut oil (containing almost

116   only saturated fatty acids). All diets contained heme iron (0.094% w/w) to catalyze lipid peroxidation.

117   All animal experiments were performed in accordance with EU directive 2010/63/EU and approved by

118   the local Animal Care and Use Committee of Toulouse Midi-Pyrénées (agreement TOXCOM/0006/FG).

119   **Sample preparation**

120   Urine samples were allowed to thaw at room temperature. Aliquots of 500 µL were prepared for each

121   urine sample and diluted in 500 µL of mobile phase A (95% H_2O, 5% CH_3OH, 0.1% CH_3CO_2H). After

122   dilution, the aliquots were vortex-mixed and centrifuged at 10,000 rpm for 5 minutes. The

123   supernatants were transferred into vials to be directly used for analyses. This sample preparation

124   protocol was previously developed for mass spectrometric detection of urinary metabolites of

125   xenobiotics, including conjugated metabolites.[30]

126   **Liquid chromatography and mass spectrometry analyses**

127   Analyses were performed using ultra performance liquid chromatography (UPLC) (ACQUITY, Waters

128   Manchester, UK) coupled to a quadrupole time-of-flight mass spectrometer (Q-ToF Synapt G2-Si,

129   Waters, Manchester, UK). A volume of 10 µL of samples were injected into a Hypersil Gold C18 (1.9

130   µm, 100 x 2.1 mm) analytical column (Thermo Fisher Scientific, Illkirch, France) at a flow rate of 0.3

131   mL/min, and maintained at 40°C. According to a previously developed chromatographic protocol[30], a

132   linear gradient program was set up with mobile phase A: 95% H2O / 5% methanol / 0.1% acetic acid,

133   and mobile phase B: 100% methanol / 0.1% acetic acid. Initial conditions were 100% of A, followed by

134   a linear gradient from 0 to 100% of B in 30 min. These conditions were held for 4 min prior to switching

135   in 1 min to the starting conditions and held for 5 min to equilibrate the column. MS^E acquisitions (*i.e.*

136   DIA mode) were achieved with electrospray ionization (ESI) in the negative mode. Parameters were

137   set-up using two standard compounds (namely DHN-MA and *N*-acetyl-*S*-phenylcysteine) as detailed in

138   the experimental section: capillary voltage 0.5 kV, sampling cone voltage 30 V, source temperature

6

139   120 °C, desolvation temperature 550 °C, cone gas flow rate 30 L/h, desolvation gas flow rate 600 L/h

140   and a trap collision energy of 15 eV for the high energy spectra. MS^E spectra were acquired with a

141   range of mass-to-charge ratio (*m/z*) set to 50 – 800. MS^3 experiments were achieved on a LTQ Orbitrap

142   XL mass spectrometer (Thermo Scientific, Les Ulis, France).

143   A quality control (QC) sample corresponding to the pool of all samples was analyzed repetitively (n =

144   7) along the injection sequence to ensure that no instrumental deviation was observed during the

145   analysis. The quality of analyses was checked by monitoring the variation the chromatographic

146   pressure (lower than 10 bars between the first and the last injection), the variation of MS signal

147   (Relative Standard Deviation (RSD) of signal area of 8.6%), retention time (RSD of 0.15%) and mass

148   measurement accuracy (lower than 5 ppm) based on the tryptophan signal detected at 3.2 min.

149   **Data processing**

150   Data from MS^E experiments were processed with the UNIFI® software (Waters, Manchester, UK).

151   Extraction of data from full scan mass spectra was carried out using XCMS offline software[31] with

152   centwave algorithm[32] (ppm = 10, peakwidth = (10,70), snthresh = 10, noise = 2000, bw = 5, mzwid =

153   0.01). To avoid urine dilution variation among samples data were normalized using Probabilistic

154   Quotient Normalization.[33] All data analysis steps were performed using workflow4metabolomics, a

155   collaborative portal dedicated to metabolomics data processing.[34]

156   Statistical analyses were carried out using SIMCA software v15 (Umetrics, Umeå, Sweden). Results

157   were examined using unsupervised principal component analysis (PCA) in order to check the validity

158   of acquisition and to detect potential outliers. Projection to latent structure discriminant analysis

159   modeling (PLS-DA) was then carried out to find out diet discriminant features. The PLS-DA Q^2

160   parameter (fraction of samples correctly predicted by the model) was used to assess the quality of

161   models. Models with $Q^2 > 0.4$ were considered as valid. For valid models, a permutation test was

162   performed to assess the robustness of models. For valid and robust models, significant features were

163   selected by their variable importance on projection (VIP). A feature displaying a VIP > 1 was considered

164   significant.

7

165   **RESULTS AND DISCUSSION**

166   **Method development**

167   To setup ionization parameters for the profiling of MACs, two standards were used. The first one

168   corresponds to the reduced conjugate between *N*-acetylcysteine and 4-HNE, namely DHN-MA. Since

169   this compound is generated from lipid peroxidation, it is representative of structures we would like to

170   detect. The second standard corresponds to a smaller structure, which displays no heteroatom other

171   than those of the *N*-acetylcysteine moiety, namely *N*-acetyl-*S*-phenylcysteine, the conjugate between

172   a phenyl group and *N*-acetylcysteine. This compound could be considered as representative of smaller

173   and less ionizable compounds.

174   UPLC coupled with HRMS through ESI is an analytical approach particularly suited for the qualitative

175   and quantitative analysis of urinary metabolites.[5] ESI in the negative mode gave the most intense

176   signal, due to the carboxylic acid function of the mercapturate that easily undergoes deprotonation.

177   Fragment ions were observed in the full MS spectrum of standards even with no collision energy

178   applied into the collision cell of the mass spectrometer. The [M-H]⁻ ion of DHN-MA was detected at

179   *m/z* 320.1531, but another intense ion was observed at *m/z* 191.1111, corresponding to the loss of

180   129 Da, representative of the *N*-acetylcysteine moiety. The same phenomenon was observed with *N*-

181   acetyl-*S*-phenylcysteine. This fragmentation was caused by an excess of internal energy of ions coming

182   from the desolvation conditions of the electrospray ion source and the conditions of transfer of the

183   ions into the Triwave and StepWave cells of the Synapt mass spectrometer. Nevertheless, this

184   fragmentation has to be limited to increase the signal of the deprotonated ions of MACs, and therefore

185   to increase the sensitivity of the method. For that purpose, we decreased the excess of internal energy

186   during the steps of ionization / desolvation and ion transfer by limiting the acceleration of ions into

187   the different cells of the Synapt mass spectrometer where remaining gas was present, *i.e.* into the

188   StepWave cell for the last step of desolvation and into the Triwave cell for the transfer of ions.

189   We based our profiling method on the property of MACs to undergo a particular fragmentation during

190   the collision induced dissociation (CID) process, leading to a neutral loss of $C_5H_7NO_3$ 129.0426 Da,

8

191   corresponding to the cleavage of the thioether bond as already mentioned in previous works. [24–28] In

192   this study, this fragmentation pattern was investigated from seven MAC standard compounds

193   originating from lipid peroxidation products conjugated with glutathione, namely 4-hydroxynonan-1-

194   ol mercapturic acid (DHN-MA), 4-hydroxyoctan-1-ol-MA, 4-hydroxyheptan-1-ol-MA, 4-hydroxyhexan-

195   1-ol-MA (DHH-MA), 4-hydroxynonanal-MA, 4-hydroxyoctanal-MA and 4-hydroxyheptanal-MA, as well

196   as the standard of N-acetyl-S-phenylcysteine. Results summarized in Table 1 show that all MACs

197   displayed the neutral loss of $C_5H_7NO_3$ 129.0426 Da. As an example, in the case of DHN-MA detected at

198   a retention time (Rt) of 13.2min, the neutral loss of 129.0426 Da was observed with a resulting

199   fragment ion at m/z 191.1106. Consecutive losses of H_2O and CH_2O led to the formation of m/z

200   173.1000 and 143.0898 ions. The complementary fragment ion $[C_5H_7NO_3\text{-}H]^-$ detected at m/z

201   128.0352, was also previously observed for three metabolites of B(a)P[35] and used as multiple reaction

202   monitoring transition (MRM) for detecting some MACs. [36] However, this ion was observed only in the

203   MS/MS spectra of DHH-MA and DHN-MA, and with a weak relative abundance (< 3%).

204   **Table 1:** UHPLC-ESI-HRMS/MS of MAC standards, achieved at a collision energy of 15 eV.

MAC	m/z	Rt (min)	Neutral Formula	Fragment Ions (Relative Abondance)
4-hydroxyheptanal-MA	290.1067	7.74	C12H21NO5S	290.1061 (20) 161.0637 (53) 143.0532 (100) 125.0426 (3) 115.0579 (25)
4-hydroxyoctanal-MA	304.1223	10.67	C13H23NO5S	304.1219 (23) 175.0792 (68) 157.069 (100) 129.0739 (27)
4-hydroxynonanal-MA (HNE-MA)	318.138	13.18	C14H25NO5S	318.1383 (16) 189.0946 (25) 171.0839 (100) 143.0880 (17)
4-hydroxyheptanol-MA	292.1223	7.35	C12H23NO5S	292.1219 (30) 163.079 (100) 145.049 (34) 130.963 (10) 115.0583 (39)
4-hydroxyoctanol-MA	306.138	10.27	C13H25NO5S	306.1373 (27) 177.0949 (100) 159.0847 (23) 129.0741 (32)
4-hydroxyhexanol-MA (DHH-MA)	278.1068	4.47	C11H21NO5S	278.1062 (20) 149.0637 (100) 131.053 (38) 128.0346 (3) 101.0424 (42)
4-hydroxynonanol-MA (DHN-MA)	320.15374	13.21	C14H27NO5S	320.1536 (4) 191.1106 (100) 173.1000 (16) 143.0898 (44) 128.0352 (2)
N-acetylphenylcysteine	238.0543	9.92	C11H13NO3S	109,0112 (100)

205

206   We applied a data-independent acquisition (DIA) process allowing the fragmentation of all ions. In the

207   Waters' Q-ToF instruments, the DIA mode is called MS^E and is based on the continuous switching

208   between a low-energy CID scan and a higher energy CID scan without any precursor ion selection. The

9

209   first scan is used to detect the precursor ion, whereas the second scan is used to detect the fragment

210   ions.[37] Data are then processed using the UNIFI® software to associate the two scans, and to build

211   product ion spectra from the collected data. Within these data, the software also offers the possibility

212   to screen every ions giving a particular neutral loss. The neutral loss tolerance was set at 5 mDa as it

213   was the value which gave the most notable results without being too large. The signal threshold of the

214   low energy scan was set at 2,000 counts to minimize the signals mixed to the background noise

215   whereas the signal threshold of the high energy scan was set at 20 counts. At the end, only candidates

216   displaying a neutral loss or a specific fragment ion detected with a mass accuracy below 10 ppm were

217   kept for subsequent processing.

218   The limit of detection (LOD) of the method was evaluated by analyzing successive dilutions of DHN-

219   MA and *N*-acetyl-*S*-phenylcysteine standard solutions prepared in blank urine samples. A signal ratio

220   of 3 was observed at concentrations of 5 ng/mL and 10 ng/mL for DHN-MA and *N*-acetyl-*S*-

221   phenylcysteine, respectively. Although the dynamic range of the detector is limited when working in

222   the profile mode, it can be increased by using the dynamic range extension (DRE) in the centroid mode.

223   Since the centroid mode is not compatible with UNIFI®, a parallel untargeted acquisition of data in the

224   centroid mode should be performed for quantitative purposes. Thus, according to the workflow

225   displayed in Figure 2, all samples were analyzed by UPLC-ESI-HRMS, and raw data were processed using

226   XCMS.[31] In parallel and using exactly the same chromatographic and ionization parameters, QC

227   samples were also analyzed by UPLC-ESI-HRMS[E] to detect MACs. Features of MACs were then

228   annotated into the XCMS dataset to allow their statistical analyses using unsupervised or supervised

229   statistical tools.

230   In DIA mode, no precursor ion is selected and fragmentation patterns are built *in-silico*. Thus, false

231   positive MACs might be detected by the profiling of the considered neutral loss. A first possible origin

232   of artefactual detection could be chromatography. However, since features detected by DIA are

233   matched to features detected by XCMS, only features displaying chromatographic characteristics in

234   agreement with parameters used for XCMS (i.e. signal to noise ratio, peak width, peak resolution) are

10

235   kept. The second origin of potential false positive MACs could be the non-specificity of the

236   fragmentation (i.e., neutral loss of $C_5H_7NO_3$ 129.0426 Da not specific of MACs), or if the deconvolution

237   algorithm of DIA is not enough robust to align the right fragment ion with the right precursor ion.

238   However, since next steps of the method aim at highlighting discriminant features with statistical tools,

239   and then identifying them with targeted MS/MS, false positive MACs will be eliminated at this last

240   step.
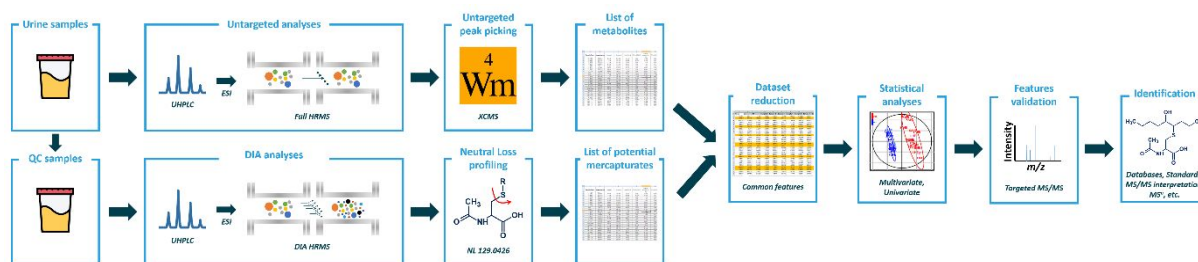
242   **Figure 1.** Workflow of the untargeted profiling of mercapturic acid conjugates.

243   **Application**

244   This method was validated on a proof-of-concept application on urine samples coming from rats fed

245   diets containing representative lipid peroxidation prone fatty acids expected to yield various

246   glutathione conjugates, further metabolized into MACs. Thus, the global profiling method of MACs

247   should be more adapted to detect MACs by comparison with an untargeted metabolomics approach.

248   Since lipid peroxidation products depend on their precursor unsaturated fatty acid, three different

249   diets were selected. The first one was based on hydrogenated coconut oil known to contain almost

250   only saturated fatty acids and which should produce no MACs (except those possibly observed coming

251   from endogenous peroxidation), the second one was based on fish oil containing long chain omega-3

252   fatty acids, and finally the third one was based on safflower oil, which is rich in omega-6 fatty acids.

253   Thus these three contrasted diets were expected to lead to specific peroxidation products, that are

254   detoxified by conjugation with glutathione, and finally eliminated as specific MACs in urine. Urine

255   samples coming from the different diets were randomly analyzed by UPLC-ESI-HRMS. Since the

256   detection of standard MACs analyzed for the set-up of the method was more sensitive in the negative

257   ionization mode, samples were analyzed only with this mode. After data acquisition, features were

11

258   detected using XCMS. Raw data were filtered according to a blank sample of mobile phase A, to keep

259   only features whose signal intensity is at least three times higher in the QC samples than in the blank

260   samples. A total of 9614 features were detected by this untargeted metabolomics approach

261   (Supporting information, Table S1). In parallel, the QC sample was also analyzed according to our

262   designed MS^E workflow. By MS^E, eighty-two MACs candidates were detected. Twenty-six of them

263   displayed poor chromatographic characteristics, including a low signal to noise ratio, a large peak width

264   or a very low chromatographic resolution. All these false positive MACs arising from chromatography

265   were not present in the XCMS data matrix (Supporting information, Table S2) illustrating the relevant

266   data curation achieved by using a parallel processing of data using XCMS.

267   An unsupervised statistical analysis by PCA was achieved on all the features detected with XCMS in all

268   samples and in the QC. No outlier sample was detected, and a good correlation of the injections of the

269   QC sample demonstrated that no deviation has occurred along the analysis (Supporting information,

270   FigureS1). The resulting PCA shows in Figure 2A a discrimination of the fish oil diet (FO), but a weak

271   separation of coconut oil diet (CO) and safflower oil diet (SA). By comparison, the same PCA achieved

272   on features filtered thanks to our MS^E approach obviously displays a better discrimination of diets

273   (Figure 2B). Results match perfectly the expected effects of the lipid peroxidation induced by heme

274   iron according to the composition of oil in poly-unsaturated fatty acids.

12
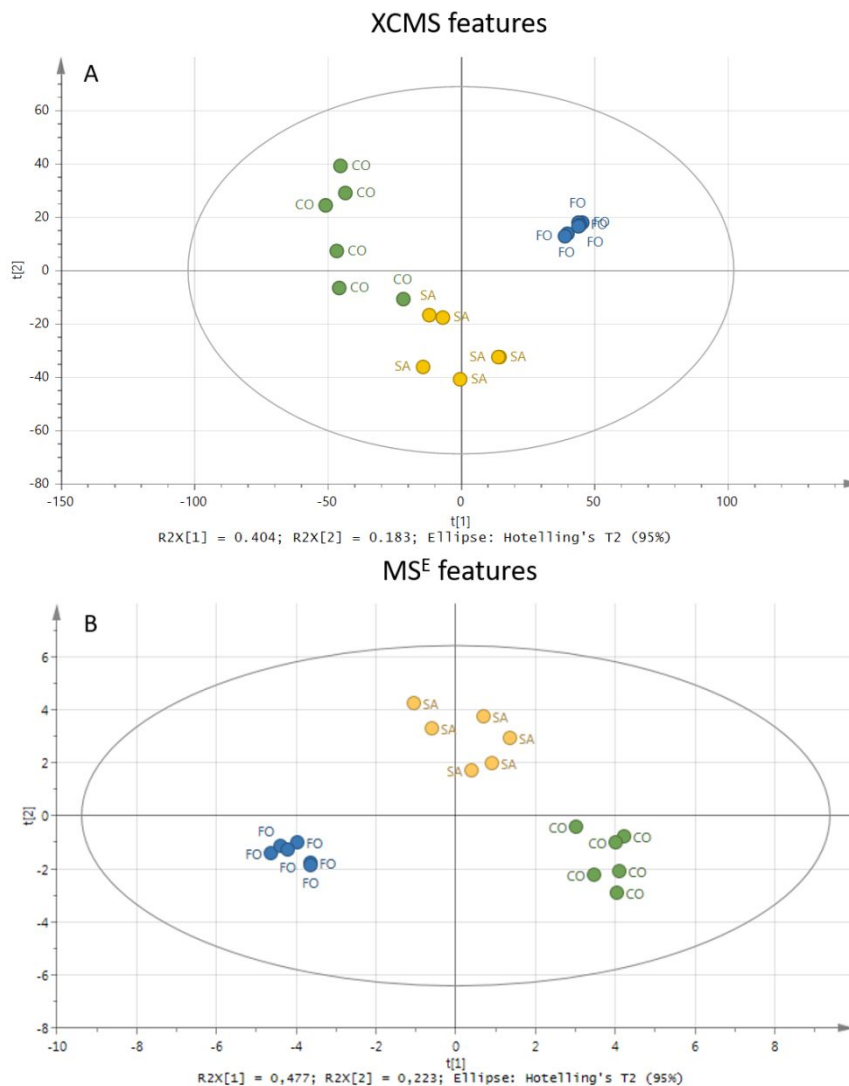
Figure 2. Principal Component Analyses of (A) all features detected with XCMS and (B) features detected by MS^E. Yellow dots (SA) represent samples from safflower oil diet, blue dots (FO) represent samples from fish oil diet, and green dots (CO) represent coconut oil diet.

To evaluate the contribution of the MS^E profiling approach to discriminate populations, PLS-DA were achieved on both dataset validated by permutation tests. Samples were discriminated according to a two components model (Q^2 = 0.94) of 3944 features with a VIP > 1 from the dataset generated by XCMS (Supporting information, FigureS2). Conversely, a two components model (Q^2 = 0.95) of 22 features with a VIP > 1 was obtained from the dataset generated by MS^E (Supporting information, FigureS3). In the XCMS dataset, discriminating MACs were ranked between the 21 and 4354 position of VIP in component 1, and between the 13 and 2929 position in component 2 (Supporting information

13

286   Table S3). This shows that the discriminating MACs were diluted into thousands of features

287   representative of other metabolites using the whole metabolomics dataset, making it very difficult to

288   identify them. At the opposite, the PLS-DA achieved on the MS^E dataset allowed to directly highlight

289   discriminating MACs and to detect two more significant MACs. This better discrimination can be

290   explained by the fact that the drastic data matrix reduction, enabling to focus the dataset only on a

291   class of metabolites of interest. The studied populations were expected to be discriminated according

292   to the lipid peroxidation products, detoxified by conjugation with glutathione and finally metabolized

293   into MACs. Therefore, by looking only at MACs, which include lipid peroxidation products conjugates,

294   the data matrix was filtered only on metabolites of interest, excluding other potential interfering

295   signals.

296   Another interesting issue of the analysis of metabolites, is the identification of discriminating

297   compounds. Since a fragmentation pattern highly specific of MACs is monitored, this identification

298   criteria can be proposed in a first attempt. To validate the loss of 129.0425 as representative of MACs,

299   targeted MS/MS analyses were attempted on the 56 MACs candidates detected in the XCMS data

300   matrix. Some MS/MS spectra could not be generated likely due to a loss of sensitivity related to the

301   decrease of the scan time which has to be set to allow numerous parallel MS/MS acquisitions, and/or

302   the weak signal of corresponding precursor ions. In all others MS/MS spectra, the expected neutral

303   loss was successfully observed, showing that no interference occurred during its detection by MS^E. To

304   assess the possible detection of a potential loss of 129.0425 from a metabolite that was not a MAC,

305   the chemical formula of each candidate was generated. Only two candidates displayed a loss of

306   129.0425 from a chemical formula bearing no sulfur atom (n230.1032T4.9 and n261.0879T5.7). The

307   list of features detected by MS^E was also matched with the HMDB database. Some features matched

308   with metabolites that are not a MAC. However, none of these other potential metabolites had MS/MS

309   spectra in HMDB displaying a $[(M - H) - 129]^-$ fragment ion.

310   Based on this proposed identification of MACs, a further hypothesis of the reactive metabolite before

311   its conjugation with glutathione can also be formulated (**Table 2**), with a particular focus on lipid

14

312   peroxidation products in this study. A chemical formula of the precursor reactive metabolite can be

313   hypothesized from the formula of the corresponding MAC, to which the *N*-acetylcysteine formula was

314   subtracted. Then, putative lipid peroxidation products were matched with the LIPID MAPS database.

315   In the case of unknowns or not well characterized lipid peroxidation products, annotation was

316   performed from bibliography of lipid peroxidation products. [29,38,39]

317   **Table 2.** Annotated MACs of lipid peroxidation products detected by UPLC-ESI-HRMS[E] in urine

318   samples of rats

XCMS feature	*m/z*	Rt (min)	[M-H]⁻ Formula	ppm	annotation of MACs	Annotation of reactive metabolite	Identification level[40]
n248.0955T6.5	248.0955	6.40	$C_{10}H_{18}NO_4S$	2.8	pentanol-MA	pentenol	3
n262.1113T9.5	262.1114	9.51	$C_{11}H_{20}NO_4S$	1.6	hexanol-MA	hexenol	3
n266.0849T13.8	266.0847	13.78	$C_{13}H_{16}NO_3S$	3.4	ethylbenzene-MA	styrene	3
n274.0746T6	274.0737	5.44	$C_{11}H_{16}NO_5S$	6.6	ethyllactone-MA	hydroxyhexenoic ac	3
n276.0905T10	276.0908	10.02	$C_{11}H_{18}NO_5S$	1.0	4-hydroxyhexanal-MA (HHE-MA)	4-hydroxyhexenal (HHE)	2
n276.1271T12.5	276.1270	12.50	$C_{12}H_{22}NO_4S$	1.8	heptanol-MA	heptenol	3
n278.1054T4.6	278.1059	4.52	$C_{11}H_{20}NO_5S$	3.1	4-hydroxyhexanol-MA (DHH-MA)	4-hydroxyhexenol (DHH)	1
n278.1054T5.6	278.1062	4.64	$C_{11}H_{20}NO_5S$	2.0	hydroxyhexanol-MA	hydroxyhexenol	3
n288.1269T13.2	288.1271	13.17	$C_{13}H_{22}NO_4S$	1.5	octanal-MA	octenal	3
n288.1269T12.5	288.1269	12.81	$C_{13}H_{22}NO_4S$	2.1	octanal-MA	octenal	3
n288.1271T11.5	288.1268	11.50	$C_{13}H_{22}NO_4S$	2.3	octanal-MA	octenal	3
n290.106T6.2	290.1057	6.07	$C_{12}H_{20}NO_5S$	3.9	hydroxyheptanal-MA	hydroxyheptenal	3
n290.1425T15.2	290.1425	15.22	$C_{13}H_{24}NO_4S$	2.0	octanol-MA	octenol	3
n304.0855T4.2	304.0854	4.54	$C_{12}H_{18}NO_6S$	2.0	hydroxypropyllactone-MA	4,7-dihydroxyheptenoic ac	3
n306.1019T4.7	306.1014	5.12	$C_{12}H_{20}NO_6S$	1.7	hydroxyheptanoic ac-MA	hydroxyheptenoic ac	3
n314.1433T14.4	314.1424	14.45	$C_{15}H_{24}NO_4S$	2.1	decenal-MA	decadienal	3
n318.1374T10.6	318.1375	10.70	$C_{14}H_{24}NO_5S$	1.9	hydroxynonenol-MA	hydroxynondienol	3
n320.117T7.1	320.1170	7.20	$C_{13}H_{22}NO_6S$	1.0	dihydroxyoctanal-MA	dihydroxyoctenal	3
n320.1529T12.9	320.1530	13.07	$C_{14}H_{26}NO_5S$	2.3	4-hydroxynonanol-MA (DHN-MA)	4-hydroxynonenol (DHN)	1
n336.1115T3.6	336.1114	3.41	$C_{13}H_{22}NO_7S$	2.3	dihydroxyoctanoic ac-MA	dihydroxyoctenoic ac	3
n362.1272T6.4	362.1274	6.34	$C_{15}H_{24}NO_7S$	1.5	wCOOH-hydroxydecanal-MA	wCOOH-hydroxydecenal	3

319

320   An interesting feature was detected at *m/z* 320.1529 and Rt = 13.07 min. This metabolite displayed a

321   *m/z* ratio consistent with a $[C_{14}H_{27}NO_5S-H]^-$ ion with a precision of 2.3ppm. Four fragment ions were

322   detected in its MS/MS spectrum (Figure 3B) *at m/z* 191.1100, 173.0997, 143.0894 and 128.0346.

15

323   Relative abundances of these ions were 100%, 23%, 52% and 2%, respectively, which were highly

324   similar with those of standard DHN-MA (Figure 3A, Table1). These two independent and orthogonal

325   data (i.e. retention time and MS/MS spectrum) comparable with a standard analyzed under identical

326   experimental conditions allowed us to identify this metabolite as DHN-MA at a level 1 of identification,

327   in full concordance with the nomenclature of identification proposed by the metabolomics standards

328   initiative (MSI).[40] Interestingly, the consecutive fragmentation of the $[(M - H) - 129]^-$ ion of DHN-MA

329   produced the m/z 143.0894 fragment ion by losses of H_2O and CH_2O. This loss of CH_2O could be

330   representative of the primary hydroxyl function of DHN-MA, which could give some information on

331   the structure of others MACs.
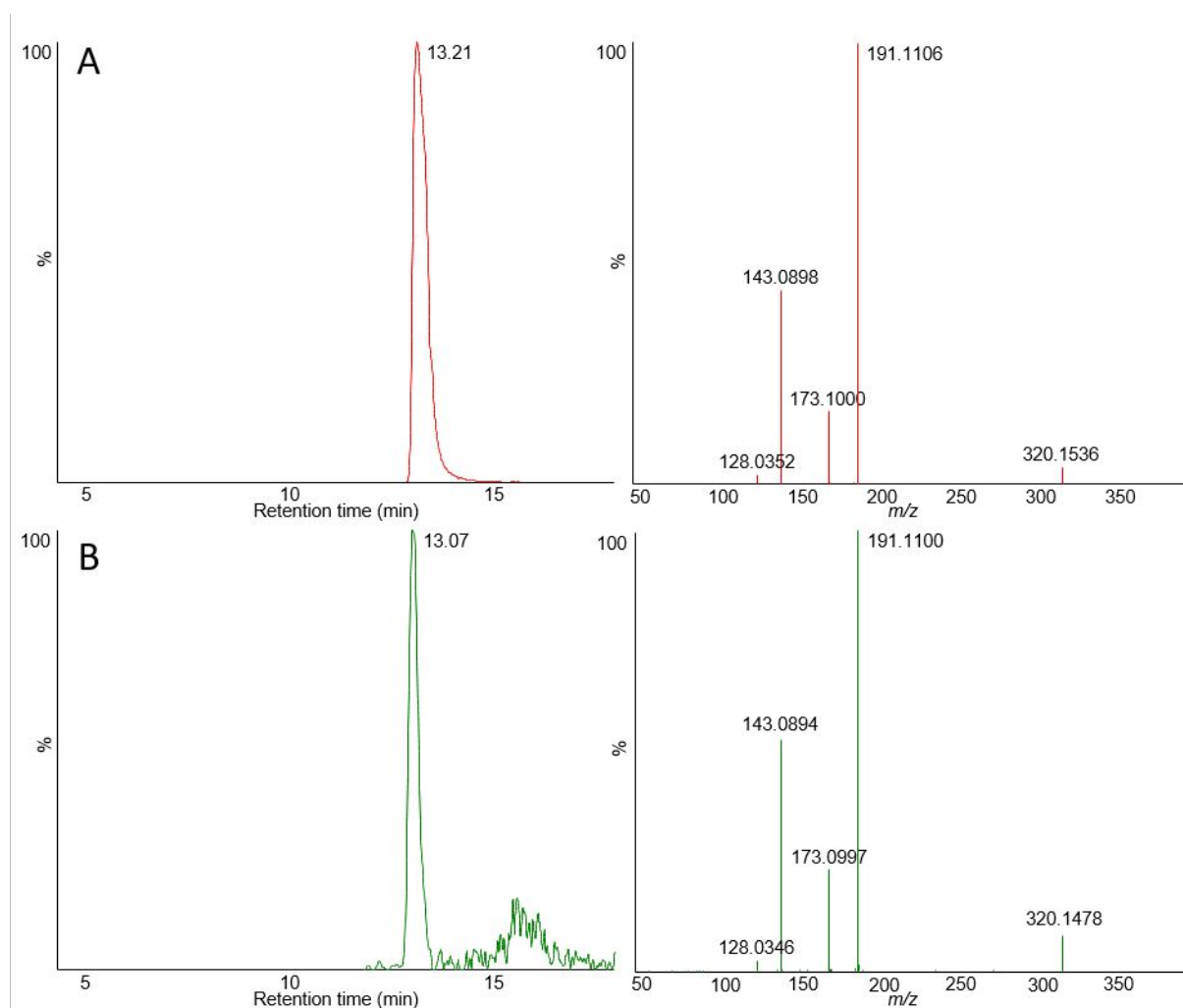
332

333   **Figure 3:** Extracted ion chromatogram and product ion spectrum at a collision energy of 15 eV, of (A)

334   the standard of DHN-MA, and (B) DHN-MA detected in urine samples.

16

335 Related to DHN-MA, the mercapturate conjugate coming from the glutathione conjugation of HNE

336 (HNE-MA), before its metabolization into DHN-MA, could also be annotated (n318.1374T10.6 in Table

337 2). However, its targeted MS/MS spectrum (Supporting information, Table S2) and its retention time

338 did not match with synthetized standard of HNE-MA (Table 1). The consecutive fragmentation of the

339 [(M - H) - 129]$^-$ ion of the standard produced the *m/z* 143.0888 fragment ion by losses of H_2O and CO.

340 This loss of CO could be representative of the aldehyde function of HNE-MA. By comparison, the

341 consecutive fragmentation of the [(M - H) - 129]$^-$ ion of the unknown n318.1374T10.6 produced the

342 *m/z* 141.0749 fragment ion by losses of H_2O and CH_2O. This observation, which is similar with DHN-

343 MA, suggests that this unknown MAC may include a primary hydroxyl function, another hydroxyl

344 function and an unsaturation, which can be a ring or a double bond.

345 Whereas DHN-MA is originating from ω-6 polyunsaturated fatty acids, ω-3 ones are known to lead to

346 the formation of 4-hydroxyhexenal (HHE), which can be conjugated with glutathione to form HHE-MA.

347 [41] HHE-MA can be metabolized similarly to HNE-MA to generate the 4-hydroxyhexanal-MA (DHH-MA),

348 which was detected at *m/z* 278.1054 and Rt = 4.52 min. This latter identification was confirmed at level

349 1 by analysis of the corresponding standard (Supporting information, FigureS4), which displayed the

350 same retention time and fragmentation pattern. The mercapturate conjugate coming from the

351 glutathione conjugation of HHE (HHE-MA), before its metabolization into DHH-MA, could also be

352 annotated (n276.0905T10 in Table 2). Based on its MS/MS spectra (Supporting information, Table S2)

353 and the biological context, the HHE-MA was putatively identified (level 2, according to MSI [40]). The *m/z*

354 290.1057 ion detected at Rt = 6.1 min (Supporting information, Table S2) was not attributed to 4-

355 hydroxyheptanal-MA, based on the MS/MS spectrum and Rt of the corresponding standard (Table 1).

356 Some annotated MACs displayed a high degree of unsaturation, which can correspond to double bonds

357 or rings. This latter possibility has already been described as lactone structures for lipid peroxidation

358 products.[39] For example, the metabolite detected at *m/z* 304.0854 and Rt = 4.5 min corresponds to a

359 conjugate formed between *N*-acetylcysteine and a structure displaying 7 carbon atoms, 3 oxygen

360 atoms, and 2 double bond equivalents. Since it is likely that this metabolite is a product of lipid

361   peroxidation, one unsaturation may be involved in a carbonyl function at the carbon in position one.

362   Then the second unsaturation can be either a carbon-carbon double bond, or another carbonyl

363   function. It is also possible that a dihydroxylated acid alken, hydroxylated in particular at position 4 can

364   be conjugated as a dihydroxylated heptanoic acid mercapturate, which could further undergo a

365   condensation to generate a lactone compound, like the hydroxypropylactone, according to previously

366   described metabolic processes for HNE. [38,39]

367   As observed on the MS/MS spectra of standards (Table 1), MACs display poor fragmentation rates,

368   which limits available information for unknowns identification. Neutral loss profiling was used to give

369   a first step of identification (i.e. MAC), and then statistics on particular population highlighted some

370   particular metabolites to have another hypothesis of identification (i.e. lipid peroxidation products).

371   Based on these hypotheses and since standard MACs are not commercially available, seven chemical

372   syntheses were achieved, among which five did not validate corresponding putative annotations. Some

373   consecutive fragmentations could occur from the $[(M - H) - 129]^-$ fragment ion, but the weak signal of

374   the precursor ion prevented their detection in many cases (Supporting information, Table S3). The use

375   of MS^3 experiments could be an alternative solution to get more structural information. However, the

376   analysis of the samples on a LTQ Orbitrap XL mass spectrometer led to the detection of only DHH-MA,

377   hydroxynonenol-MA, DHN-MA, dihydroxyoctanal-MA and dihydroxyoctanoic ac-MA, and the

378   corresponding MS^3 spectra displayed only a loss of water.

379   **CONCLUSIONS**

380   Urinary MACs are originated from detoxification conjugates between glutathione and reactive

381   electrophilic compounds that are able to bind to biomolecules, such as DNA and proteins and to induce

382   deleterious effects. These compounds can be electrophilic as such or be the result of the bioactivation

383   of xenobiotics to which we are exposed. Therefore, by monitoring MACs into urine, it is possible to

384   monitor their precursor electrophilic metabolites and by extension, the molecules from which these

385   metabolites are produced and which can be considered as toxicologically relevant compounds. The

386   global profiling of MACs combining the detection of known and unknown MACs by using MS^E, and their

18

387   relative quantification, pave the way for addressing new perspectives in toxicology. The application of

388   this method to the study of lipid peroxidation catalyzed by heme iron, allowed highlighting various

389   unknown structures of reactive lipid peroxidation products, which may be implicated in the promotion

390   of colorectal cancer, similarly to 4-HNE [42]. This detection of unknown potentially reactive metabolites

391   was greatly facilitated by the simplification of statistical analyses due to dataset reduction provided by

392   the specific monitoring of metabolites of interest using the MS^E profiling. Although our workflow

393   suffers from some complexity because of the difficulty to obtained large amount of quantitative data

394   with the software we used for DIA processing, this approach could be adapted to other mass

395   spectrometers, DIA approaches, or fast data dependent acquisitions.

396   This case study was only focused on the study of MACs to demonstrate the proof of concept. However,

397   the approach could be applied to monitor other classes of metabolites and markers, such as conjugates

398   with glucuronic acid, sulfate, cysteine, glutathione, as well as DNA and RNA adducts as recently

399   published,[43] which are all displaying characteristic neutral losses.

400   Furthermore, it is noteworthy that this method is providing not only the profiling of MACs by MS^E, but

401   also in parallel an untargeted analysis of the metabolome by HRMS, in the same samples. Indeed, an

402   untargeted metabolomics analysis by reversed phase liquid chromatography coupled with HRMS using

403   electrospray ionization is able to detect amino acids, organic acids, polyols, nucleosides, indoles, etc.

404   [44], which can give access to the metabolome modifications induced by the studied diets. Therefore,

405   this method allows characterizing a series of toxicologically relevant compounds in one hand, as well

406   as the study of their effects on the metabolome in the other hand, in the same analysis of samples.

407   This may represent a valuable way to link exposure to toxics and possible health adverse outcomes.

408   **ACKNOWLEDGMENTS**

19

413   **ASSOCIATED CONTENT**

414   **Supporting Information**

415   Table S1: Data matrix obtained form UPLC-ESI-HRMS using XCMS; Table S2: Candidates of MACs

416   detected in the XCMS matrix and validated by targeted MS/MS; Table S3: VIP of the PLS-DA of the

417   XCMS dataset and the MS^E dataset; Figure S1: Principal Component Analysis of all features detected

418   with XCMS; Figure S3: Projection to latent structure discriminant analysis modeling (PLS-DA) of all

419   features detected with XCMS; Figure S3: Projection to latent structure discriminant analysis modeling

420   (PLS-DA) of features detected by MSE; Figure S4: **:** Extracted ion chromatograms of DHH-MA obtained

421   by UPLC-ESI-HRMS from (A) the standard of DHH-MA and (B) urine samples. Corresponding product

422   ion spectra obtained by electrospray in the negative mode from (C) the standard of DHH-MA and (D)

423   urine samples.

REFERENCES

(1)   Lu, C.; Barr, D. B.; Pearson, M. A.; Waller, L. A. Dietary Intake and Its Contribution to

Longitudinal Organophosphorus Pesticide Exposure in Urban/Suburban Children. *Environ.*

Health Perspect. **2008**, *116* (4), 537–542. https://doi.org/10.1289/ehp.10912.

(2)   Pestka, J. J. Deoxynivalenol: Mechanisms of Action, Human Exposure, and Toxicological

Relevance. *Arch. Toxicol.* **2010**, *84* (9), 663–679. https://doi.org/10.1007/s00204-010-0579-8.

(3)   Cascella, M.; Bimonte, S.; Barbieri, A.; Del Vecchio, V.; Caliendo, D.; Schiavone, V.; Fusco, R.;

Granata, V.; Arra, C.; Cuomo, A. Dissecting the Mechanisms and Molecules Underlying the

Potential Carcinogenicity of Red and Processed Meat in Colorectal Cancer (CRC): An Overview

on the Current State of Knowledge. *Infect. Agent. Cancer* **2018**, *13* (1), 3.

https://doi.org/10.1186/s13027-018-0174-9.

(4)   Wild, C. P. Complementing the Genome with an "Exposome": The Outstanding

Challenge of Environmental Exposure Measurement in Molecular Epidemiology. *Cancer*

Epidemiol. Biomarkers Prev. **2005**, *14* (8), 1847–1850. https://doi.org/10.1158/1055-9965.EPI-

05-0456.

(5)   Jamin, E. L.; Bonvallot, N.; Tremblay-Franco, M.; Cravedi, J. P.; Chevrier, C.; Cordier, S.;

Debrauwer, L. Untargeted Profiling of Pesticide Metabolites by LC-HRMS: An Exposomics Tool

for Human Exposure Evaluation. *Anal. Bioanal. Chem.* **2014**, *406* (4), 1149–1161.

https://doi.org/10.1007/s00216-013-7136-2.

(6)   Ashby, J.; Tennant, R. W. Chemical Structure, Salmonella Mutagenicity and Extent of

Carcinogenicity as Indicators of Genotoxic Carcinogenesis among 222 Chemicals Tested in

Rodents by the U.S. NCI/NTP. *Mutat. Res.* **1988**, *204* (1), 17–115.

(7)   Turesky, R. J. Mechanistic Evidence for Red Meat and Processed Meat Intake and Cancer Risk:

A Follow-up on the International Agency for Research on Cancer Evaluation of 2015. *Chim. Int.*

J. Chem. **2018**, *72* (10), 718–724. https://doi.org/10.2533/chimia.2018.718.

(8)   Hemeryck, L. Y.; Van Hecke, T.; Vossen, E.; De Smet, S.; Vanhaecke, L. DNA Adductomics to

21

450 Study the Genotoxic Effects of Red Meat Consumption with and without Added Animal Fat in

451 Rats. *Food Chem.* **2017**, *230*, 378–387. https://doi.org/10.1016/j.foodchem.2017.02.129.

452 (9) Sinha, R.; Knize, M. G.; Salmon, C. P.; Brown, E. D.; Rhodes, D.; Felton, J. S.; Levander, O. A.;

453 Rothman, N. Heterocyclic Amine Content of Pork Products Cooked by Different Methods and

454 to Varying Degrees of Doneness. *Food Chem. Toxicol.* **1998**, *36* (4), 289–297.

455 https://doi.org/10.1016/S0278-6915(97)00159-2.

456 (10) Santarelli, R.; Pierre, F.; Corpet, D. Processed Meat and Colorectal Cancer: A Review of

457 Epidemiologic and Experimental Evidence. *Nutr. Cancer* **2008**, *60* (2), 131–144.

458 https://doi.org/10.1080/01635580701684872.

459 (11) de La Pomélie, D.; Santé-Lhoutellier, V.; Gatellier, P. Mechanisms and Kinetics of Heme Iron

460 Nitrosylation in an in Vitro Gastro-Intestinal Model. *Food Chem.* **2018**, *239*, 86–93.

461 https://doi.org/10.1016/J.FOODCHEM.2017.06.092.

462 (12) Guéraud, F.; Taché, S.; Steghens, J.-P.; Milkovic, L.; Borovic-Sunjic, S.; Zarkovic, N.; Gaultier, E.;

463 Naud, N.; Héliès-Toussaint, C.; Pierre, F.; et al. Dietary Polyunsaturated Fatty Acids and Heme

464 Iron Induce Oxidative Stress Biomarkers and a Cancer Promoting Environment in the Colon of

465 Rats. *Free Radic. Biol. Med.* **2015**, *83*, 192–200.

466 https://doi.org/10.1016/J.FREERADBIOMED.2015.02.023.

467 (13) Surya, R.; Héliès-Toussaint, C.; Martin, O. C.; Gauthier, T.; Guéraud, F.; Taché, S.; Naud, N.;

468 Jouanin, I.; Chantelauze, C.; Durand, D.; et al. Red Meat and Colorectal Cancer: Nrf2-

469 Dependent Antioxidant Response Contributes to the Resistance of Preneoplastic Colon Cells

470 to Fecal Water of Hemoglobin- and Beef-Fed Rats. *Carcinogenesis* **2016**, *37* (6), 635–645.

471 https://doi.org/10.1093/carcin/bgw035.

472 (14) IJssennagger, N.; Rijnierse, A.; de Wit, N.; Jonker-Termont, D.; Dekker, J.; Müller, M.; van der

473 Meer, R. Dietary Haem Stimulates Epithelial Cell Turnover by Downregulating Feedback

474 Inhibitors of Proliferation in Murine Colon. *Gut* **2012**, *61* (7), 1041–1049.

475 https://doi.org/10.1136/gutjnl-2011-300239.

476   (15)   Carlsen, C. U.; Møller, J. K. S.; Skibsted, L. H. Heme-Iron in Lipid Oxidation. *Coord. Chem. Rev.*

477   **2005**, *249* (3–4), 485–498. https://doi.org/10.1016/J.CCR.2004.08.028.

478   (16)   Sesink, A. L. A.; Termont, D. S. M. L.; Kleibeuker, J. H.; Van der Meer, R. Red Meat and Colon

479   Cancer: The Cytotoxic and Hyperproliferative Effects of Dietary Heme. *Cancer Res.* **1999**, *59*

480   (22), 5704–5709.

481   (17)   Bastide, N. M.; Pierre, F. H. F.; Corpet, D. E. Heme Iron from Meat and Risk of Colorectal

482   Cancer: A Meta-Analysis and a Review of the Mechanisms Involved. *Cancer Prev. Res.* **2011**, *4*

483   (2), 177–184. https://doi.org/10.1158/1940-6207.CAPR-10-0113.

484   (18)   Chevolleau, S.; Noguer-Meireles, M.-H.; Jouanin, I.; Naud, N.; Pierre, F.; Gueraud, F.;

485   Debrauwer, L. Development and Validation of an Ultra High Performance Liquid

486   Chromatography-Electrospray Tandem Mass Spectrometry Method Using Selective

487   Derivatisation, for the Quantification of Two Reactive Aldehydes Produced by Lipid

488   Peroxidation, HNE (4-Hydroxy-2(E)-Nonenal) and HHE (4-Hydroxy-2(E)-Hexenal) in Faecal

489   Water. *J. Chromatogr. B. Analyt. Technol. Biomed. Life Sci.* **2018**, *1083*, 171–179.

490   https://doi.org/10.1016/j.jchromb.2018.03.002.

491   (19)   Guéraud, F. 4-Hydroxynonenal Metabolites and Adducts in Pre-Carcinogenic Conditions and

492   Cancer. *Free Radic. Biol. Med.* **2017**, *111*, 196–208.

493   https://doi.org/10.1016/J.FREERADBIOMED.2016.12.025.

494   (20)   Kuiper, H. C.; Miranda, C. L.; Sowell, J. D.; Stevens, J. F. Mercapturic Acid Conjugates of 4-

495   Hydroxy-2-Nonenal and 4-Oxo-2-Nonenal Metabolites Are in Vivo Markers of Oxidative Stress.

496   *J. Biol. Chem.* **2008**, *283* (25), 17131–17138. https://doi.org/10.1074/jbc.M802797200.

497   (21)   Rossin, D.; Calfapietra, S.; Sottero, B.; Biasi, F. HNE and Cholesterol Oxidation Products in

498   Colorectal Inflammation and Carcinogenesis. *Free Radic. Biol. Med.* **2017**, *111*, 186–195.

499   https://doi.org/10.1016/J.FREERADBIOMED.2017.01.017.

500   (22)   Hinchman, C. A.; Ballatori, N. Glutathione Conjugation and Conversion to Mercapturic Acids

501   Can Occur as an Intrahepatic Process. *J. Toxicol. Environ. Health* **1994**, *41* (4), 387–409.

23

502   https://doi.org/10.1080/15287399409531852.

503   (23)   Mathias, P. I.; B'Hymer, C. A Survey of Liquid Chromatographic–Mass Spectrometric Analysis

504   of Mercapturic Acid Biomarkers in Occupational and Environmental Exposure Monitoring. *J.*

505   *Chromatogr. B* **2014**, *964*, 136–145. https://doi.org/10.1016/J.JCHROMB.2014.02.057.

506   (24)   Scholz, K.; Dekant, W.; Völkel, W.; Pähler, A. Rapid Detection and Identification of N-Acetyl-L-

507   Cysteine Thioethers Using Constant Neutral Loss and Theoretical Multiple Reaction

508   Monitoring Combined with Enhanced Product-Ion Scans on a Linear Ion Trap Mass

509   Spectrometer. *J. Am. Soc. Mass Spectrom.* **2005**, *16* (12), 1976–1984.

510   https://doi.org/10.1016/j.jasms.2005.08.003.

511   (25)   Wagner, S.; Scholz, K.; Donegan, M.; Burton, L.; Wingate, J.; Völkel, W. Metabonomics and

512   Biomarker Discovery: LC-MS Metabolic Profiling and Constant Neutral Loss Scanning

513   Combined with Multivariate Data Analysis for Mercapturic Acid Analysis. *Anal. Chem.* **2006**, *78*

514   (4), 1296–1305. https://doi.org/10.1021/ac051705s.

515   (26)   Jian, W.; Yao, M.; Zhang, D.; Zhu, M. Rapid Detection and Characterization of in Vitro and

516   Urinary N -Acetyl-L-Cysteine Conjugates Using Quadrupole-Linear Ion Trap Mass Spectrometry

517   and Polarity Switching. *Chem. Res. Toxicol.* **2009**, *22* (7), 1246–1255.

518   https://doi.org/10.1021/tx900035j.

519   (27)   Panuwet, P.; Nguyen, J. V.; Kuklenyik, P.; Udunka, S. O.; Needham, L. L.; Barr, D. B.

520   Quantification of Atrazine and Its Metabolites in Urine by On-Line Solid-Phase Extraction–

521   High-Performance Liquid Chromatography–Tandem Mass Spectrometry. *Anal. Bioanal. Chem.*

522   **2008**, *391* (5), 1931–1939. https://doi.org/10.1007/s00216-008-2102-0.

523   (28)   Koszucka, A.; Nowak, A. Thermal Processing Food-Related Toxicants: A Review. *Crit. Rev. Food*

524   *Sci. Nutr.* **2018**, 1–18. https://doi.org/10.1080/10408398.2018.1500440.

525   (29)   Alary, J.; Debrauwer, L.; Fernandez, Y.; Cravedi, J.-P.; Rao, D.; Bories, G. 1,4-Dihydroxynonene

526   Mercapturic Acid, the Major End Metabolite of Exogenous 4-Hydroxy-2-Nonenal, Is a

527   Physiological Component of Rat and Human Urine. *Chem. Res. Toxicol.* **1998**, *11* (2), 130–135.

24

528   https://doi.org/10.1021/tx970139w.

529 (30) Jamin, E. L.; Bonvallot, N.; Tremblay-Franco, M.; Cravedi, J.-P.; Chevrier, C.; Cordier, S.;

530   Debrauwer, L. Untargeted Profiling of Pesticide Metabolites by LC–HRMS: An Exposomics Tool

531   for Human Exposure Evaluation. *Anal. Bioanal. Chem.* **2014**, *406* (4), 1149–1161.

532   https://doi.org/10.1007/s00216-013-7136-2.

533 (31) Smith, C. A.; Want, E. J.; O'Maille, G.; Abagyan, R.; Siuzdak, G. XCMS: Processing Mass

534   Spectrometry Data for Metabolite Profiling Using Nonlinear Peak Alignment, Matching, and

535   Identification. *Anal. Chem.* **2006**, *78* (3), 779–787. https://doi.org/10.1021/ac051437y.

536 (32) Tautenhahn, R.; Böttcher, C.; Neumann, S. Highly Sensitive Feature Detection for High

537   Resolution LC/MS. *BMC Bioinformatics* **2008**, *9* (1), 504. https://doi.org/10.1186/1471-2105-

538   9-504.

539 (33) Dieterle, F.; Ross, A.; Schlotterbeck, G.; Senn, H. Probabilistic Quotient Normalization as

540   Robust Method to Account for Dilution of Complex Biological Mixtures. Application in 1H NMR

541   Metabonomics. *Anal. Chem.* **2006**, *78* (13), 4281–4290. https://doi.org/10.1021/ac051632c.

542 (34) Giacomoni, F.; Le Corguille, G.; Monsoor, M.; Landi, M.; Pericard, P.; Petera, M.; Duperier, C.;

543   Tremblay-Franco, M.; Martin, J.-F.; Jacob, D.; et al. Workflow4Metabolomics: A Collaborative

544   Research Infrastructure for Computational Metabolomics. *Bioinformatics* **2015**, *31* (9), 1493–

545   1495. https://doi.org/10.1093/bioinformatics/btu813.

546 (35) Yang, Y.; Griffiths, W. J.; Sjövall, J.; Gustafsson, J.-Å.; Rafter, J. Liquid Chromatography-Mass

547   Spectrometry with Collision-Induced Dissociation of Conjugated Metabolites of

548   Benzol[a]Pyrene. *J. Am. Soc. Mass Spectrom.* **1997**, *8* (1), 50–61.

549   https://doi.org/10.1016/S1044-0305(96)00136-5.

550 (36) Frigerio, G.; Mercadante, R.; Polledri, E.; Missineo, P.; Campo, L.; Fustinoni, S. An LC-MS/MS

551   Method to Profile Urinary Mercapturic Acids, Metabolites of Electrophilic Intermediates of

552   Occupational and Environmental Toxicants. *J. Chromatogr. B* **2019**, *1117*, 66–76.

553   https://doi.org/10.1016/J.JCHROMB.2019.04.015.

554   (37)   Plumb, R. S.; Johnson, K. A.; Rainville, P.; Smith, B. W.; Wilson, I. D.; Castro-Perez, J. M.;

555   Nicholson, J. K. UPLC/MSE; a New Approach for Generating Molecular Fragment Information

556   for Biomarker Structure Elucidation. *Rapid Commun. Mass Spectrom.* **2006**, *20* (13), 1989–

557   1994. https://doi.org/10.1002/rcm.2550.

558   (38)   Alary, J.; Fernandez, Y.; Debrauwer, L.; Perdu, E.; Guéraud, F. Identification of Intermediate

559   Pathways of 4-Hydroxynonenal Metabolism in the Rat. *Chem. Res. Toxicol.* **2003**, *16* (3), 320–

560   327. https://doi.org/10.1021/tx025671k.

561   (39)   Alary, J.; Debrauwer, L.; Fernandez, Y.; Paris, A.; Cravedi, J.-P.; Dolo, L.; Rao, D.; Bories, G.

562   Identification of Novel Urinary Metabolites of the Lipid Peroxidation Product 4-Hydroxy-2-

563   Nonenal in Rats. *Chem. Res. Toxicol.* **1998**, *11* (11), 1368–1376.

564   https://doi.org/10.1021/tx980068g.

565   (40)   Sumner, L. W.; Amberg, A.; Barrett, D.; Beale, M. H.; Beger, R.; Daykin, C. A.; Fan, T. W.-M.;

566   Fiehn, O.; Goodacre, R.; Griffin, J. L.; et al. Proposed Minimum Reporting Standards for

567   Chemical Analysis Chemical Analysis Working Group (CAWG) Metabolomics Standards

568   Initiative (MSI). *Metabolomics* **2007**, *3* (3), 211–221. https://doi.org/10.1007/s11306-007-

569   0082-2.

570   (41)   Winter, C. K.; Segall, H. J.; Jones, A. D. Distribution of Trans-4-Hydroxy-2-Hexenal and Tandem

571   Mass Spectrometric Detection of Its Urinary Mercapturic Acid in the Rat. *Drug Metab. Dispos.*

572   *15* (5), 608–612.

573   (42)   Bastide, N. M.; Chenni, F.; Audebert, M.; Santarelli, R. L.; Tache, S.; Naud, N.; Baradat, M.;

574   Jouanin, I.; Surya, R.; Hobbs, D. A.; et al. A Central Role for Heme Iron in Colon Carcinogenesis

575   Associated with Red Meat Intake. *Cancer Res.* **2015**, *75* (5), 870–879.

576   https://doi.org/10.1158/0008-5472.CAN-14-2554.

577   (43)   Guo, J.; Villalta, P. W.; Turesky, R. J. Data-Independent Mass Spectrometry Approach for

578   Screening and Identification of DNA Adducts. *Anal. Chem.* **2017**, *89* (21), 11728–11736.

579   https://doi.org/10.1021/acs.analchem.7b03208.

26

580   (44)   Contrepois, K.; Jiang, L.; Snyder, M. Optimized Analytical Procedures for the Untargeted

581   Metabolomic Profiling of Human Urine and Plasma by Combining Hydrophilic Interaction

582   (HILIC) and Reverse-Phase Liquid Chromatography (RPLC)–Mass Spectrometry. *Mol. Cell.*

583   *Proteomics* **2015**, *14* (6), 1684–1695. https://doi.org/10.1074/mcp.M114.046508.

584

27